ACS Photonics

Article

pubs.acs.org/journal/apchd5

Experimental Evidence for Axial Anisotropy beyond the Diffraction Limit Induced with a Bias Voltage Plasmonic Nanoantenna and Longitudinal Optical Near-Fields in Photoreactive Polymer Thin Films

Sergey S. Kharintsev,*[,†] Alexander I. Fishman,[†] Sergei G. Kazarian,[‡] Ildar R. Gabitov,[§] and Myakzyum Kh. Salakhov[†]

[†]Department of Optics and Nanophotonics, Institute of Physics, Kazan Federal University, Kremlevskaya, 16, Kazan, 420008, Russia

[‡]Department of Chemical Engineering, Imperial College London, London SW7 2AZ, United Kingdom

[§]Department of Mathematics, University of Arizona, 617 N. Santa Rita Avenue P.O. Box 210089, Tucson, Arizona 85721-0089, United States

ABSTRACT: This work highlights a mechanism for inducing axial anisotropy in side-chain nitroazobenzene (NAB) polymer thin films based on the combined effect of both local dc electrical poling and the longitudinal optical near-field. We show that highly anisotropic NAB chromophores are effectively oriented in the glassy environment under optical pumping with 632.8 nm excitation wavelength, which is out of the absorption band of chromophores. Axial anisotropy across the polymer thin film and its non-centrosymmetric behavior beyond the diffraction limit are experimentally rendered with tip-enhanced Raman scattering microscopy and scanning Kelvin probe microscopy.

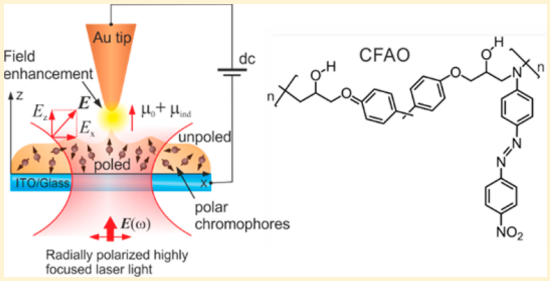

KEYWORDS: *optical near-field poling, dc electrical field poling, optical anisotropy, tip-enhanced Raman scattering, light-induced molecular motion, trans−cis photoisomerization*

Over the past several decades azobenzene-functionalized polymers have been the subject of extensive studies due to their unique feature of being readily driven with light and/or applied electrical field.[1−4] Underlying azobenzene chromophores have found a wide variety of potential applications in photomechanics and optoelectronics such as optical switches,[5] surface relief gratings,[6−8] frequency conversion,[9−11] optical near-field sensing,[12] and molecule recognition.[4] The physical mechanism of all light-induced effects in photoreactive polymers is based on the π-electron delocalization of the elongated aromatic structures, which is followed by appropriate electron-acceptor/donor ring substitution.[1] A crucial peculiarity of chromophore moieties is strong anisotropy in dipole moment and polarizability. These enable chromophores to become oriented both optically and electrically. Traditionally, polar chromophores embedded in rigid polymer matrixes are aligned by applying dc high-voltage discharge corona poling above the glass transition temperature, T_g.[13] The orientation polarization makes the polymer thin film axially anisotropic and non-centrosymmetric, and thus a nonlinear optical activity appears.[14] To locally orient the chromophores over the extent of several nanometers, scanning probe microscopy (SPM) is normally introduced.[15,16] In this case, the macroscopic heating of the polymer results in rapid reorientation of aligned chromophores. In order to locally support the induced anisotropy, one can use a focused laser beam, which is coupled to an optical nanoantenna, or a thermo/conductive atomic force microscopy (AFM) cantilever.[2,15] At modest laser intensities (~mW/cm^2), the mobility of the surface polymer layer increases due to reversible *trans−cis* photoisomerazation of azobenzene chromophores via predominately the inversion mechanism at temperatures below T_g.[17] Both the angular burning hole (ABH) effect[14,18] and optical-field gradient forces[19] lead to the formation of an anisotropic optical fingerprint on the film surface when it is exposed to light with a wavelength within the absorption band of the chromophore. Photoinduced polymer mass transport due to translation diffusion contributes to the optical anisotropy as well. With higher laser intensities (~kW/cm^2), thermal effects start to play a role, which, on one hand, soften the polymer film but, on the other hand, can inevitably result in bleaching and degradation.[20,21] A reversible polarization-dependent surface pattern has been a convincing argument in favor of polymer integrity and stability as reported everywhere.[3,8,22] In the laser-assisted heating mode a bias voltage (bv) scattering-type AFM cantilever creates the optical anisotropy beneath the tip apex and holds this state down to room temperature.[2,3]

In this paper, the axial optical anisotropy induced and probed with a bv plasmonic gold nanoantenna in photoreactive polymer thin films on the subwavelength scale is experimentally demonstrated. Longitudinal optical near-fields are generated by highly focused laser light (~kW/cm2) with 632.8 nm excitation wavelength, which is out of the absorption band of polar

Received: June 25, 2014
Published: September 17, 2014

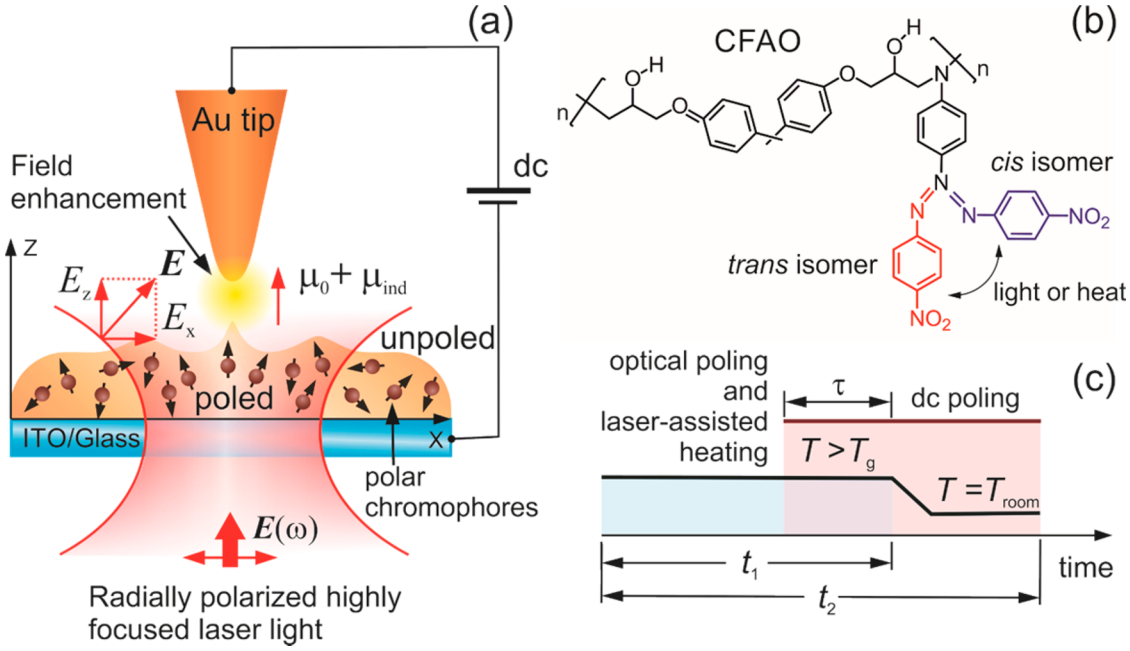

Figure 1. (a) Sketch of polar anisotropic chromophores' orientation with a bv gold nanoantenna illuminated with highly focused laser light; (b) chemical structure of a NAB chromophore covalently attached to a polymer backbone (CFAO); (c) schematic illustration of optical and dc electrical poling.

chromophores. We provide evidence for anisotropic and non-centrosymmetric behavior of the NAB polymer thin film exposed to optical near-field poling with tip-enhanced Raman scattering (TERS) microscopy and scanning Kelvin probe method.

EXPERIMENTAL SECTION

Figure 1a shows a principal scheme of an experimental setup for inducing optical anisotropy on the subwavelength scale. All measurements were performed with a commercially available versatile SPM-equipped confocal optical spectrometer, NTEGRA SPECTRA (NT-MDT, Russia). A dc high-voltage supply is applied between a conical gold nanoantenna driven by a shear force feedback mechanism, and an indium−tin-oxide (ITO)-coated glass plate served as a flat counter electrode. A 100× oil immersion objective (NA =1.49) focuses the linearly polarized light onto the sample. Radially polarized light was designed by passing the light through four zero-order quartz retarder plates with proper crystal directions (0°, 90°, +45°, −45°). In the inverted mode backscattered irradiation is collected by the same objective, decomposed with a 600 grooves/mm grating, and registered with a Newton EMCCD camera (ANDOR, Ireland) cooled to −85 °C.

TERS spectra were recorded with a cone-shaped plasmonic gold tip (or optical antenna). It is coupled with a laser beam to excite localized surface plasmons at the tip apex. The gold tip was prepared by dc-pulsed voltage, electrochemically etching at V_{down} = 1.5 V and V_{up} = 1.9 V in a mixture of fuming hydrochloric acid (HCl, 37%), 2-propanol ($CH_3CH(OH)CH_3$, 96%), and distilled water in a volume proportion of 5:3:2.[23,24]

In our study we used a side-chain 4-amino-4′-nitro-azobenzene chromophore covalently attached to the polymer backbone of two epoxy-based oligomers containing hydroxyl groups (CFAO) (T_g = 130 °C, M_w = 24 200) (Figure 1b).[13] In such a configuration, the dipole moment of the chromophore is aligned transverse to the main chain backbone (T-polymer) and provides a large quadratic nonlinearity with its good thermal stability.[25] This is in contrast to azobenzene chromophores incorporated in the main chain backbone (L-polymer). In particular, a large quadratic nonlinear optical activity with a d_{33} of ∼62 pm/V not taking into account self-absorption at the second-harmonic frequency was achieved for the T-polymer.[26] Figure 1b shows two possible geometrical configurations of NAB chromophores in the T-polymer, often referred to as *trans*- and *cis*-forms, which are reversibly interconverted via rotation or inversion mechanisms under exposure to light and/or heat.[1]

A solution was prepared by dissolving 5 wt % CFAO compound in 1 mL of cyclohexanone. A 70 nm thick CFAO film was produced by spin-casting 5 μL of a CFAO solution onto an ITO/glass substrate at 10 000 rpm for 3 min. To remove the remaining solvent, the film was annealed at 130 °C and 10 mbar for 2 h.

Plasmon-enhanced longitudinal excitation causes both orientational and translational diffusion of chromophore moieties due to strong axial optical gradient forces. These make the polymer anisotropic only, since polar chromophores are arranged with respect to the *z*-axis in a random way. In addition, the near-field heats an area beneath the tip apex and orientational mobility appears under dc electrical field impact. In this case, we observe local one-directional alignment of chromophore moieties, provided that the area of interest is under above T_g thermal load. Importantly, a local dc electric field results in a non-centrosymmetrical behavior of chromophores and, therefore, large nonlinear activity is expected. In our experiment, we used an approach shown schematically in Figure 1c. The polymer thin film is exposed to laser light for time t_1, and the dc electric field is delayed by a magnitude of $t_1 - \tau$ for time t_2. Electrical poling is held until the sample is cooled to room temperature to fix chromophores toward the dc electrical field. Evidently, characteristic times of t_1, t_2, and τ depend dramatically on polymer film thickness, substrate

dx.doi.org/10.1021/ph5002318 | ACS Photonics 2014, 1, 1025−1032

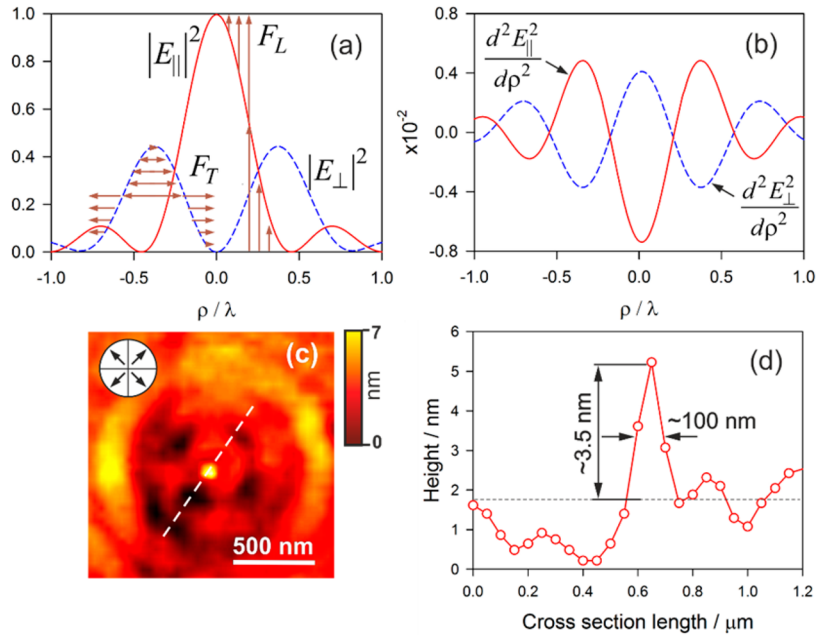

Figure 2. (a) Transverse $|E_\perp|^2$ and longitudinal $|E_{||}|^2$ electrical field components of highly squeezed radially polarized laser light; (b) the second derivative of transverse and longitudinal electrical components; (c) AFM topography of a CFAO polymer film surface when a scattering-type AFM cantilever assisted the 532 nm laser impact; (d) cross section of the surface deformation relief along the dashed line marked in panel c.

thermal conductivity, and the polymer glass temperature and should be empirically found.

RESULTS AND DISCUSSION

Optical Poling of Anisotropic Chromophores. A resultant frequency-dependent dipole moment of NAB chromophore in an optical field $\boldsymbol{E}(\omega)$ reads as

$$\boldsymbol{\mu} = \boldsymbol{\mu}_0 + \boldsymbol{\mu}_{\text{ind}} = \vec{\mu}_0\mathbf{n} + [\vec{\alpha} + \vec{\alpha}'g]\mathbf{E}(\omega) \quad (1)$$

where $\boldsymbol{\mu}_0$ and $\boldsymbol{\mu}_{\text{ind}}$ are permanent and induced dipole moments, $\vec{\mu}_0$ is a permanent dipole tensor, $\boldsymbol{n}$ is a unit vector along the z-axis, $\vec{\alpha}$and $\vec{\alpha}'$ are polarizability tensors without and with an optical antenna, respectively, and g is a scalar field enhancement factor. A density functional theory numerical calculation gives rise to the following permanent dipole moment (units: Debye, D) and static polarizability tensors (units: cubic angström, Å^3) for the NAB chromophore in the *trans*-state[27]

$$\vec{\mu}_0 = \begin{bmatrix} 0.49 & 0 & 0 \\ 0 & 0.10 & 0 \\ 0 & 0 & 12.02 \end{bmatrix} \text{D}$$

$$\text{and } \vec{\alpha}_0 = \begin{bmatrix} 8.11 & 0 & 0 \\ 0 & 65.00 & 0 \\ 0 & 0 & 79.31 \end{bmatrix} \text{Å}^3 \quad (2)$$

These relationships confirm the highly anisotropic nature of NAB chromophores. Note that the permanent and induced dipole moments are not co-directional. A structure of the tensor $\vec{\alpha}'$ is dependent on the geometry of an optical antenna and its permittivity. Orientation polarization of anisotropic chromophores can be induced with optical fields (referred to as a "direct" mechanism) due to highly repetitive, little constant torques $\mathbf{M} = \vec{\alpha}\cdot\mathbf{E} \times \mathbf{E}$, provided that *trans*- and *cis*-isomers are in a thermodynamic equilibrium and the concentration of *trans*-isomers exceeds significantly that of *cis*-isomers. Alternative mechanisms concern the ABH effect and angular redistribution (referred to as "indirect mechanisms") in which back *cis*–*trans* photoisomerization gives rise to the accumulation of *trans*-chromophores oriented perpendicularly to the light polarization and thus no longer being photoreactive.[14] One should emphasize that these mechanisms compete with each other. Indeed, the effect of the direct mechanism is maximal when chromophores are primarily aligned to be transverse to the light polarization, whereas the indirect mechanism contributes to the anisotropy with a probability $P(\theta) \approx \cos^2\theta$ (where θ is an angle between the dipole moment and the polarization).[28] Importantly, an induced dipole moment is less than a permanent dipole moment by 2 orders of magnitude even at a high electrical field of ~10^7 V/m. In the presence of a nanoantenna the strength of confined optical fields increases by g times, values of that fall into the range from 10 to 100, and, finally, the permanent and induced dipole moments get comparable. One should bear in mind that the induced dipole moments are aligned along the light polarization, whereas permanent dipoles are oriented toward a dc electric field to meet the non-centrosymmetric state of the T-polymer.

Photoinduced optical transverse and/or longitudinal anisotropy can be recognized with a surface pattern that is caused by large-scale light-induced polymer motion.[3,20,29] This phenomenon is well studied from the viewpoint of the influence of polarization, a focus position with respect to a sample of incident irradiation and its power, on the pattern morphology.[20,22] However, the underlying mechanism remains unclear so far. The optical gradient force model allows one to describe the behavior of a surface mobile layer of ~10 nm in depth at room temperature.[29] *Trans*–*cis* photoisomerization makes the polymer surface viscoelastic and mobile due to an anomalous increase of free volume.[29] Another mechanism deals with local annealing via absorption at room temperature of the whole polymer. Photoinduced thermal effects become negligible for ultrathin films (<10 nm in thickness) and high heat conductivity of a substrate (>10 W/m·K) at high intensities of the laser irradiation. Light-driven deformation on the film

dx.doi.org/10.1021/ph5002318 | ACS Photonics 2014, 1, 1025−1032

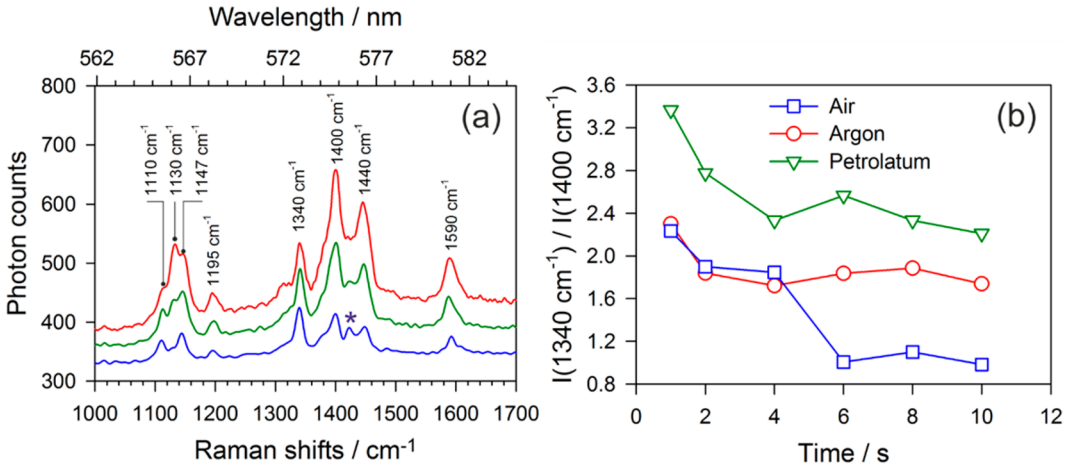

Figure 3. (a) Resonance Raman spectra of a CFAO polymer film exposed to 532 nm linearly polarized laser light with a power of 1.5 kW/cm^2 and exposure times of 5 s (blue), 10 s (green), and 15 s (red) (the asterisk indicates the 1425 cm^{-1} line). (b) Kinetics of a ratio of intensities at 1340 and 1400 cm^{-1} measured in the presence of air, argon, and petrolatum at a light power of 7 kW/cm^2.

surface beyond the diffraction limit can be achieved with a highly focused (NA >1) radially polarized laser light.[3,30] A doughnut-shaped transverse component of the electrical field $|E_\perp|^2$, calculated 2 nm around a focal plane as shown in Figure 2a,[30] leads to a 180° shifted surface profile; $S(\rho) \approx d^2|E_\perp|^2/d\rho^2$ ($\rho = (x,y)$) (Figure 2b), which is analogous to a two-beam interference-induced pattern studied by Bian et al. in detail.[30] The on-axis longitudinal component of the electrical field $|E_\parallel|^2$ exceeds the transverse component by ~2 times the magnitude[31] and may contribute to the polymer migration as well. Because the diffraction-limited spot diameters in the lateral ρ and longitudinal z directions are 250 and 620 nm, respectively, the longitudinal force F_L gradient effect is significantly less than that for the transverse force F_T. On the other hand, those chromophore moieties, which are anchored along the z-axis, strongly absorb longitudinal fields and the ABH orientation effect comes into play. Finally, it leads to the in-plane arrangement of chromophores. It is important to note that the film thickness influences the balance between transverse/longitudinal optical forces and anisotropic fluidic forces, and it leads to distinguishable morphologies from a dip to protrusion at the core of the optical pattern.[2] To reinforce the axial optical gradient, a scattering or plasmonic type optical antenna should be brought into the longitudinal lobe. The formation of a subwavelength protrusion beneath the tip apex was for the first time demonstrated by Davy et al.[32] Figure 2c shows the AFM image of a surface pattern engraved by both the AFM cantilever operating in the tapping mode and the 532 nm radially polarized light at a moderate laser power of ~200 W/cm^2 and an exposure time of 60 s. It follows from a cross section along a dashed line, given in Figure 2d, that the height of the protrusion and its full width at half-height are equal to ~3.5 and ~100 nm, respectively. The subwavelength peculiarity at the core of the surface pattern confirms the fact that the longitudinal force, F_L, is predominant. Four dark depletion zones around the core comes from the four-section radial retarder and optical force gradient. This is in good agreement with the theoretical data shown in Figure 2b. A bulging ring beyond the depletion spots is a consequence of the diffraction-limited laser beam and the transverse polymer migration in the direction from the optical axis.

Raman Spectroscopy as a Probe of Optical Anisotropy. Resonance Raman spectroscopy supports our knowledge about the integrity and stability of NAB chromophores at different light loads. Figure 3a shows resonance Raman spectra of the CFAO thin film exposed to 532 nm linearly polarized laser light with a power of 1.5 kW/cm^2 and exposure times of 5, 10, and 15 s. A closer examination points out the appearance of a spectral band at 1130 cm^{-1} that grows noticeably with the optical pumping. Note that this peak exists when 632.8 nm irradiation is used, but it does not appear when the film is exposed to 785 nm irradiation until the polymer is photobleached. Finding Raman features for *cis*-isomers is infeasible because *trans*−*cis* and *cis*−*trans* isomerization exhibit picosecond time scales.[1] This means that the 1130 cm^{-1} peak is most likely caused by photochemical oxidation in air. To support this assumption, we repeated our experiment with argon blowdown and petrolatum and found that the 1130 cm^{-1} band is not observed under the same conditions. A crucial peculiarity is the fact that the peaks at 1110 and 1340 cm^{-1}, which are assigned to the phenyl-NO_2 stretch and the NO_2 symmetric stretch,[33,34] reasonably drop in intensity with laser power. Note that changes in intensity of the 1130 and 1340 cm^{-1} peaks are opposite to each other; that is, when the 1130 cm^{-1} peak increases, the 1340 cm^{-1} peak diminishes and vice versa. When the peak saturation is achieved in time, we observe a decrease of the total spectrum that is stipulated by photobleaching and degradation. The observable peaks at 1147, 1400, and 1440 cm^{-1} are the result of a phenyl-NN, NN, and NO stretches, whereas peaks at 1195 and 1590 cm^{-1} are assigned to the CH in-plane bend and CC stretch, respectively.[33,34] A spectral anomaly at 1425 cm^{-1} remains unchangeable on increasing the irradiation time, and it is independent of the light power. More importantly, no changes in intensities of the peaks are observed in the presence of argon or petrolatum under high light loads until the polymer is chemically destroyed. To quantitatively characterize the kinetics of the 1130 cm^{-1} band, we used a ratio of intensities at 1340 and 1400 cm^{-1} as a measure of degradation, since these are well resolved and very sensitive to the high intensities of laser irradiation. Figure 3b shows the kinetics of this magnitude in different environments—air, argon, and petrolatum—at a higher laser power of 7 kW/cm^2. Even though the petrolatum

dx.doi.org/10.1021/ph5002318 | ACS Photonics 2014, 1, 1025−1032

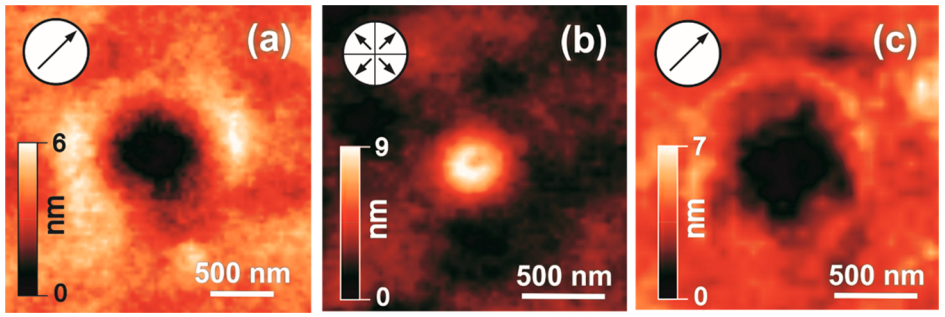

Figure 4. AFM topography of a surface pattern on the 70 nm thick CFAO polymer thin film exposed to linearly (a, c) and radially (b) polarized 632 nm excitation at a power of 1 kW/cm^2 (a, b) and 26 kW/cm^2 (c) and an exposure time of 120 s (a, b) and 10 s (c).

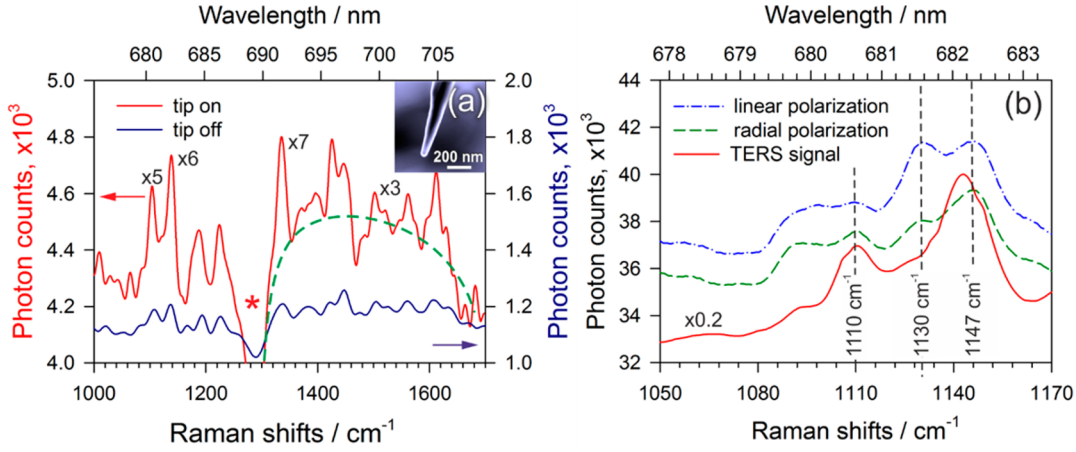

Figure 5. (a) Raman spectra of the azobenzene polymer film when a gold tip, shown in the inset, is on (red curve) and off (blue curve) under 632.8 nm longitudinal excitation. The asterisk indicates a dip in fluorescence spectra shown in Figure 3a, and the dashed green curve represents the fluorescence enhancement. Numerals indicate enhancement factors in the tip-on mode. (b) Raman spectra of the CFAO polymer film excited with linearly and radially polarized 632.8 nm laser light and a tip-enhanced Raman scattering spectrum (red curve) (reduced by 5 times).

environment functions better as a upper protective layer in contrast to inert gas, it obstructs focusing a laser beam on the petrolatum/polymer interface because the refractive indexes are close to each other. We clearly see that argon and petrolatum reasonably prevent a destruction of the polymer. Photoinduced oxidation at high light intensities in the air environment is a multistep and ambiguous process that requires a meticulous study.

Figure 4a and b show AFM images of photoinduced surface patterns exposed to light with 632.8 nm excitation wavelength at a power of 1 kW/cm^2 and an exposure time of 120 s. Polarization-dependent fingerprints confirm nanoscale polymer migration that is most likely caused by the optical gradient forces model. This is explicitly supported by the formation of both a two-lobe pattern (Figure 4a) and an on-axis protrusion (Figure 4b) induced with linearly and radially polarized light, respectively. The UV−vis absorption spectrum with a peak intensity of 490 nm gives the following absorption coefficient values: $\alpha_{532\ nm}$ = 1.30 μm^{-1} and $\alpha_{633\ nm}$ = 0.06 μm^{-1} for the ∼70 nm thick CFAO film. Therefore, *trans*−*cis* isomerization plays a lesser role in facilitating fluidic properties of the polymer under laser light impact. A photoinduced blot-like pattern, engraved at a power of 24 kW/cm^2 and an exposure time of 10 s, with lateral sizes exceeding the laser spot is shown in Figure 4c. Local thermal effects destroy the polymer, and an irreversible crater normally forms. Thus, light-driven polymer nanomovement can be directly initialized with an excitation wavelength out of the absorption band.

As a result of the strongly anisotropic nature of chromophore moieties, we can probe their intrinsic molecular features and study the behavior of oriented chromophores with polarized Raman spectroscopy.[35] However, a huge fluorescence observed in the red spectral region impedes the facile determination of the Raman peaks. TERS spectroscopy enables an improvement of optical contrast by several orders of magnitude and extraction spectral information at the single-molecule level. This is a powerful tool for probing ultrathin polymer film down to molecular monolayers.[36,37] The enhanced optical field beneath the tip apex reaches values of 10^9 V/m, and thus permanent and induced dipole moments become comparable. Figure 5a displays Raman spectra of the amorphous CFAO thin film exposed to radially polarized laser irradiation without and with a plasmonic nanoantenna, referred to as a gold tip, taken at a power of 7 kW/cm^2 and an exposure time of 60 s. The inset in Figure 5a shows a scanning electron microscopy image of the 25 nm curvature radius gold tip. Despite the fact that fluorescence, displayed as a green dashed curve in Figure 5a, is also enhanced, tip-enhanced Raman peaks demonstrate more 3-fold enhancement. A singularity marked with an asterisk comes from the irregular behavior of the fluorescence. Of great interest is the fact that at giant longitudinal optical fields the 1130 cm^{-1} peak is not observed. It might be explained by the in-plane arrangement of chromophores on the film surface. To

dx.doi.org/10.1021/ph5002318 | ACS Photonics 2014, 1, 1025−1032

check this hypothesis, polarized far- and near-field Raman measurements were performed with a high spectral resolution of 0.46 cm^{-1} (1800 grooves/mm grating). Figure 5b shows that a linearly polarized excitation inevitably results in the appearance of the 1130 cm^{-1} peak, whereas it is observed to a lesser extent when the polymer film is exposed to radially polarized light. This effect becomes sharper with TERS spectroscopy due to a highly enhanced and localized longitudinal excitation (Figure 5b). It is important to stress that this peak appears again after the chromophores were optically out-of-plane oriented and a giant absorption comes into play. To this end, we conclude that TERS can be used for finding spectroscopic features in the case of chormophores whose permanent dipole moments are perpendicular to the light polarization. Otherwise, TERS causes chromophores to be photobleached or photodegraded.

Non-centrosymmetric Behavior of a CFAO Film. As mentioned above, all-optical poling aligns randomly oriented dipole moments in a preferential direction, and thus we reach only optical anisotropy. A non-centrosymmetric behavior of anisotropic chromophore moieties with large dipole moments is induced by a dc electric field. In this case, both bound and injection charges occur on the film surface exposed to light and/or a dc electric field. Kelvin probe force microscopy provides surface potential mapping of the CFAO polymer film under light and electrical loads with parameters t_1 = 300 s, τ = 60 s, t_2 = 600 s, dc voltage of −10 V, light power of ∼200 W/cm^2. We observe a positive potential at a place of interest, as shown in Figure 6a. This suggests that most of chromophores

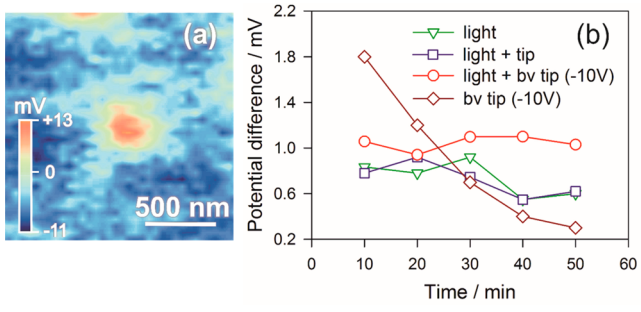

Figure 6. (a) Surface potential mapping of the CFAO polymer film influenced with 632.2 nm longitudinal excitation and tip-assisted dc electrical poling for 600 s. (b) Potential difference kinetics at a spot under various impact mechanisms.

with negatively charged NO_2 end groups face inward toward the bulk. Because of a large electrical field gradient applied between the bv tip and the ITO/glass substrate, the film surface is mainly charged via an ionic injection mechanism. To better understand the charging effect, the kinetics of the surface potential on the film surface exposed to different conditions is shown in Figure 6b. By applying a dc voltage of −10 V the induced charge essentially drops, and therefore we can conclude that this is an injection mechanism. A little remnant potential is observed when the polymer film is affected by light and tip-assisted light. A combined effect of a bv tip and light leads to a nonvanishing potential that is caused by bound charges on the near-surface of the oriented polymer film. This behavior differs noticeably from the behavior observed at the initial moment when only the bv tip is used (Figure 6b). The injection charging effect becomes negligible when the film surface is exposed to light, which evokes large-scale polymer migration on the near-surface and thus changes the equipotential surface. This means that photoinduced effects are favorable for eliminating undesirable injection charges.

TERS Probing for Axial Anisotropy. The performance of axial anisotropy beyond the diffraction limit is accomplished with the bv gold tip coupled with highly focused radially polarized light. Optical and electrical conditions impacting the CFAO polymer thin film were produced with parameters t_1 = 300 s, τ = 60 s, t_2 = 600 s, dc voltage of −10 V, excitation wavelength of 632.8 nm, and a light power of 200 W/cm^2. A photoinduced surface pattern was visualized with scanning shear force microscopy, as shown in Figure 7a. A cross section along a dashed straight line demonstrates an on-axis protrusion with the height of ∼3.3 nm and a full width at half-height of ∼200 nm. An internal dashed circle outlines the laser impact trace. The second circle shows photoinduced symmetrically positioned depleted spots due to light reflected from the tip. TERS mapping enables the phonon features of the film surface to be probed with subwavelength spatial resolution. Figure 7c and d show a 64 × 64 pixel TERS map at 1147 cm^{-1}, and Figure 7d shows the cross section along the dashed straight line. The exposure time was 0.5 s per pixel. An optical contrast at the core of the surface pattern is caused by the longitudinal excitation and correlates well with out-of-plane-oriented polymer protrusion, depicted in Figure 7a. However, unlike the topography a full width at half-height is equal to ∼100 nm, which provides evidence for axial anisotropy beyond the diffraction limit. A depletion area around the core is stipulated by in-plane-aligned chromophores that can be easily activated with linearly polarized light. Earlier Bian et al.[30] reported that the on-axis photoinduced protrusion was caused by degradation of the polymer, but the mechanism has remained unclear. The fact that the central part of the optical pattern is not bleached is demonstrated in TERS maps at 1110 cm^{-1} (Figure 7e), 1130 cm^{-1} (Figure 7f), and 1400 cm^{-1} (Figure 7g). Importantly, the 1130 cm^{-1} peak responsible for photodegradation via an oxidation mechanism is not observed. We believe that the core protrusion formation is stipulated by both in-plane and out-plane translation diffusion due to optical gradient forces. On the other hand, the maps at 1147 and 1400 cm^{-1} assigned to phenyl-NN stretch and NN stretch are similar to each other. Transverse orientation of chromophores results in optical depletion when longitudinal excitation is exerted. Thus, the tip-enhanced optical fields may be successfully used not only for making fingerprints of highly anisotropic single molecules but for studying their orientations as well. This is possible due to an optical contrast between two light polarizations states: (1) parallel and (2) perpendicular to the permanent dipole moment. Note the restrictions imposed on optical fields in an inverted optical scheme: longitudinal optical fields are confined within the extent of several nanometers, whereas transverse optical fields are diffraction limited.

CONCLUSIONS

In summary, we conclude that the axial anisotropy beyond the diffraction limit in a CFAO thin film can be induced by a bv gold tip assisted longitudinal excitation in a nondestructive fashion. Photoinduced nanoscale deformation on the thin film surface takes place when it is exposed to light with a 632.8 nm excitation wavelength, which is out of the absorption band of chromophores. We have shown that the polymer film is not photobleached via an oxidation mechanism in argon and petrolatum environments. Unfortunately, temperature control

dx.doi.org/10.1021/ph5002318 | ACS Photonics 2014, 1, 1025−1032

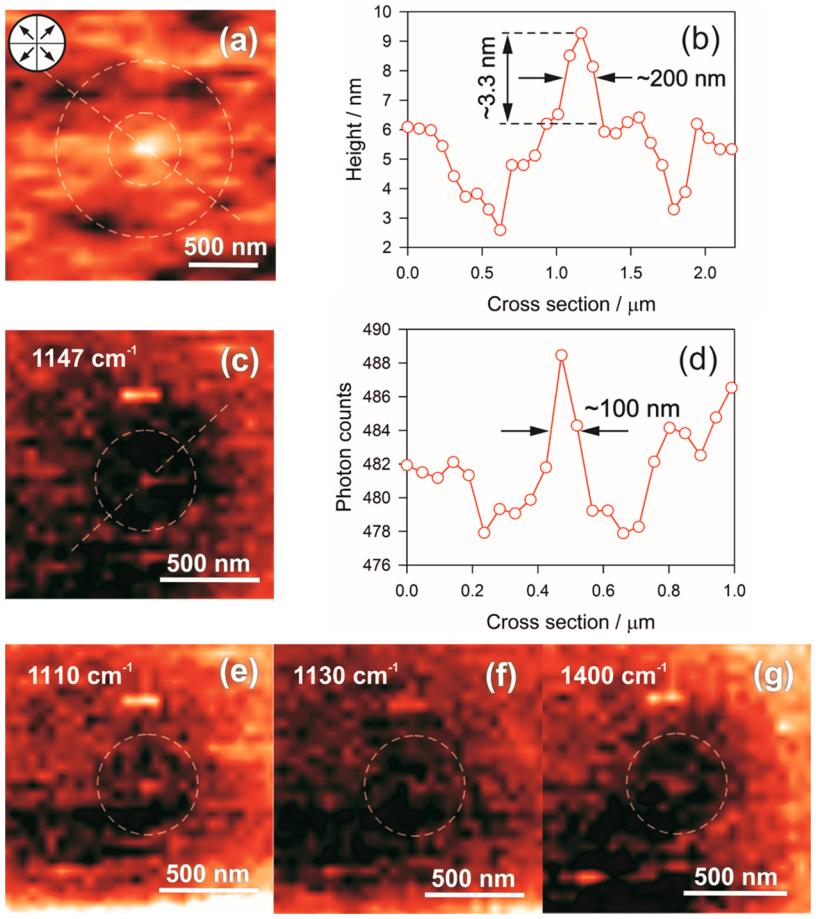

Figure 7. (a) Shear force topography and cross section along a dashed straight line (b) of the CFAO polymer film under optical and dc electrical poling during 600 s. (c) TERS mapping and cross section along a dashed straight line (d) of the CFAO polymer film at 1147 cm^{-1}. (e, f, and g) TERS mapping at 1110, 1130, and 1400 cm^{-1}, respectively.

within the laser spot remains infeasible, and, thus, the suggestion that the polar orientation occurs at temperatures below T_g seems to be unconvincing. The non-centrosymmetric behavior of the polymer film is proved with a nonvanishing surface potential that is followed by out-of-plane-oriented polar choromophores. The on-axis orientation alignment of these has been demonstrated by TERS microscopy. A highly inhomogeneous high-order laser beam leads to a nonuniform distribution of the optical anisotropy; the chromophores are out-of-plane aligned at the nanoscale core of the optical pattern and in-plane oriented in the doughnut depletion zone. Finally, the information revealed in this study can be used to aid effective fabrication of a subwavelength Bragg grating to boost the quantum yield of near-field high-order harmonic generation.[38]

AUTHOR INFORMATION

Corresponding Author

*E-mail: Sergey.Kharintsev@kpfu.ru. Tel: +7(843)2337741.

Notes

The authors declare no competing financial interest.

ACKNOWLEDGMENTS

The authors thank Prof. M. Yu. Balakina (A.E. Arbuzov Institute of Organic and Physical Chemistry KSC RAS) for helpfully preparing samples and acknowledge technical support from Artem Shalaev (NT-MDT, Russia) and Ksenia Nefedieva (Kazan Federal University). This work was financially supported by the Russian Foundation for Basic Research (no. 13-02-00758 A). S.G.K. also acknowledges research funding from the European Research Council under the European Community's Seventh Framework Programme (FP7/2007–2013)/ERC advanced grant agreement no. 227950. This work was done using equipment from the Federal Center of Shared Equipment of Kazan Federal University.

REFERENCES

(1) Mahimwalla, Z.; Yager, K. G.; Mamiya, J.; Shishido, A.; Priimagi, A.; Barrett, C. J. Azobenzene photomechanics: prospects and potential applications. *Polym. Bull.* **2012**, *69*, 967–1006.

(2) Ishitobi, H.; Nakamura, I.; Kobayashi, T.; Hayazawa, N.; Sekkat, Z.; Kawata, S.; Inouye, Y. Nanomovement of azo polymers induced by longitudinal fields. *ACS Photonics* **2014**, *1*, 190–197.

(3) Gilbert, Y.; Bachelot, R.; Royer, P.; Bouhelier, A.; Wiederrecht, G. P.; Novotny, L. Longitudinal anisotropy of the photoinduced molecular migration in azobenzene polymer films. *Opt. Lett.* **2006**, *31*, 613–618.

(4) Halabieh, R. H. El; Mermut, O.; Barrett, C. Using light to control physical properties of polymers and surfaces with azobenzene chromophores. *J. Pure Appl. Chem.* **2004**, *76*, 1445–1465.

(5) Shi, W.; Ding, Y. J.; Mu, X.; Yin, X.; Fang, C. Electro-optic and electromechanical properties of poled polymer thin films. *Appl. Phys. Lett.* **2001**, *79*, 3749.

(6) Sobolewska, A.; Bartkiewicz, S. Surface relief grating in azo-polymer obtained for s-s polarization configuration of the writing beams. *Appl. Phys. Lett.* **2012**, *101*, 193301.

(7) Garrot, D.; Lassailly, Y.; Lahlil, K.; Boilot, J. P.; Peretti. Real-time near-field imaging of photoinduced matter motion in thin solid films containing azobenzene derivatives. *J. Appl. Phys. Lett.* **2009**, *94*, 033303.
(8) Viswanathan, N. K.; Balasubramanian, S.; Li, L.; Kumar, J.; Tripathy, S. K. Surface-initiated mechanism for the formation of relief gratings on azo-polymer films. *J. Phys. Chem. B* **1998**, *102*, 6064−6070.
(9) Wang, Y.; Tai, O. Y.-H.; Wang, C. H. Second-harmonic generation in an optically poled azo-dye/polymer film. *J. Chem. Phys.* **2005**, *123*, 164704.
(10) Singer, K. D.; Sohn, J. E.; Lalama, S. J. Second harmonic generation in poled polymer films. *Appl. Phys. Lett.* **1986**, *49*, 248.
(11) Sugihara, O.; Kinoshita, T.; Okabe, M.; Kunioka, S.; Nonaka, Y.; Sasaki, K. Phase-matched second harmonic generation inpoled dye/polymer waveguide. *Appl. Opt.* **1991**, *30*, 2957−2960.
(12) Landraud, N.; Peretti, J.; Chaput, F.; Lampel, G.; Boilot, J.-P.; Lahlil, K.; Safarov, V. I. Near-field optical patterning on azo-hybrid sol−gel films. *Appl. Phys. Lett.* **2001**, *79*, 4562.
(13) Nikonorova, N. A.; Balakina, M. Y.; Fominykh, O. D.; Pudovkin, M. S.; Vakhonina, T. A.; Diaz-Calleja, R.; Yakimansky, A. V. Dielectric spectroscopy and molecular dynamics of epoxy oligomers with covalently bonded nonlinear optical chromophore. *Chem. Phys. Lett.* **2012**, *552*, 114−121.
(14) Atassi, Y.; Chauvin, J.; Delaire, J. A.; Delouis, J.-F.; Fanton-Maltey, I.; Nakatani, K. Photoinduced manipulations of photochromes in polymers: Anisotropy, modulation of the NLO properties and creation of surface gratings. *Pure Appl. Chem.* **1998**, *70*, 2157−2166.
(15) Chien, F. S.-S.; Lin, C. Y.; Hsu, C. C. Local photo-assisted poling of azo copolymer films by scanning probe microscopy. *J. Phys. D: Appl. Phys.* **2008**, *41*, 235502.
(16) Chien, F. S.-S.; Lin, C. Y.; Huang, C. R.; Chang, C. S.; Hsu, C. C. Polar orientation induced by local photo-assisted poling in azo copolymer films. *J. Opt. Soc. Am. B* **2010**, *27*, 773.
(17) Bandara, H. M. D.; Burdette, S. C. Photoisomerization in different classes of azobenzene. *Chem. Soc. Rev.* **2012**, *41*, 1809−1825.
(18) Maeda, M.; Ishitobi, H.; Sekkat, Z.; Kawata, S. Polarization storage by nonlinear orientational hole burning in azo dye-containing polymer films. *Appl. Phys. Lett.* **2004**, *85*, 351.
(19) Kumar, J.; Li, L.; Jiang, X. L.; Kim, D.-Y.; Lee, T. S.; Tripathy, S. Gradient force: the mechanism for surface relief grating formation in azobenzene functionalized polymers. *Appl. Phys. Lett.* **1998**, *72*, 2096.
(20) Ishitobi, H.; Tanabe, M.; Sekkat, Z.; Kawata, S. The anisotropic nanomovement of azo-polymers. *Opt. Express* **2007**, *15*, 652−659.
(21) Galvan-Gonzalez; Canva, M.; Stegeman, G. I.; Sukhomlinova, L.; Twieg, R. J.; Chan, K. P.; Kowalczyk, T. C.; Lackritz, H. S. Photodegradation of azobenzene nonlinear optical chromophores: the influence of structure and environment. *J. Opt. Soc. Am. B* **2000**, *17*, 1992.
(22) Ishitobi, H.; Shoji, S.; Hiramatsu, T.; Sun, H.-B.; Sekkat, Z.; Kawata, S. Two-photon induced polymer nanomovement. *Opt. Express* **2008**, *16*, 14106−14114.
(23) Kharintsev, S. S.; Rogov, A. M.; Kazarian, S. G. Nanopatterning and tuning of optical taper antenna apex for tip-enhanced Raman scattering performance. *Rev. Sci. Instrum.* **2013**, *84*, 093106.
(24) Kharintsev, S. S.; Hoffmann, G. G.; Fishman, A. I.; Salakhov, M. Kh. Plasmonic optical antenna design for performing tip-enhanced Raman spectroscopy and microscopy. *J. Phys. D: Appl. Phys.* **2013**, *46*, 145501.
(25) Tsutsumi, N.; Matsumoto, O.; Sakai, W.; Kiyotsukuri, T. Nonlinear optical polymers with dipole moment aligned transverse to main chain. *Appl. Phys. Lett.* **1995**, *67*, 2272.
(26) Vakhonina, T. A.; Sharipova, S. M.; Ivanova, N. V.; Fominykh, O. D.; Smirnov, N. N.; Yakimansky, A. V.; Balakina, M. Y.; Sinyashin, O. G. Nonlinear-optical properties of epoxyamine-based thin films. *Mendeleev Commun.* **2011**, *21*, 75−76.
(27) Fominykh, O. D.; Balakina, M. Yu. Modeling of structure and nonlinear optical activity of epoxy-based oligomers with dendritic multichromophore fragments. *Macromol. Symp.* **2012**, *316*, 52−62.
(28) Thi Kim, N. N.; Dumont, M.; Delaire, J. A.; Nakatani, K. Orientation of azo-dye molecules in polymer films, via photoisomerization: dichroism measurements and second harmonic generation. *Mol. Cryst. Liq. Cryst.* **2005**, *430*, 249−256.
(29) Barrett, C. J.; Rochon, P. L.; Natansohn, A. L. Model of laser-driven mass transport in thin films of dye-functionalized polymers. *J. Chem. Phys.* **1998**, *109*, 1505.
(30) Bian, S.; Williams, J. M.; Kim, D. Y.; Li, L.; Balasubramanian, S.; Kumar, J.; Tripathy, S. Photoinduced surface deformations on azobenzene polymer films. *J. Appl. Phys.* **1999**, *86*, 4498.
(31) Novotny, L.; Beversluis, M.; Youngworth, K.; Brown, T. Longitudinal field modes probed by single molecules. *Phys. Rev. Lett.* **2001**, *86*, 5251−5254.
(32) Davy, S.; Spajer, M. Near field optics: snapshot of the field emitted by a nanosource using a photosensitive polymer. *Appl. Phys. Lett.* **1996**, *69*, 3306.
(33) Stuart, C. M.; Frontiera, R. R.; Mathies, R. A. Excited-state structure and dynamics of cis- and trans-azobenzene from resonance raman intensity analysis. *J. Phys. Chem. A* **2007**, *111*, 12072−12080.
(34) Nowak, M.; Mccreery, R. L. Characterization of carbon/nitroazobenzene/titanium molecular electronic junctions with photoelectron and Raman spectroscopy. *Anal. Chem.* **2004**, *76*, 1089−1097.
(35) Liem, H.; Etchegoin, P.; Whitehead, K. S.; Bradley, D. D. C. Raman scattering as a probe of morphology in conjugated polymer thin films. *J. Appl. Phys.* **2002**, *92*, 1154.
(36) Xue, L.; Li, W.; Hoffmann, G. G.; Goossens, J. G. P.; Loos, J.; de With, G. High-resolution chemical identification of polymer blend thin films using tip-enhanced Raman mapping. *Macromolecules* **2011**, *44*, 2852−2858.
(37) Yeo, B.-S.; Amstad, E.; Schmid, T.; Stadler, J.; Zenobi, R. Nanoscale probing of a polymer-blend thin film with tip-enhanced Raman spectroscopy. *Small* **2009**, *5*, 952−960.
(38) Bouhelier, A.; Beversluis, M.; Hartschuh, A.; Novotny, L. Near-field second-harmonic generation induced by local field enhancement. *Phys. Rev. Lett.* **2003**, *90*, 013903.